Eastern Boundary Currents and Coastal Upwelling

S. G. H. PHILANDER AND J.-H. YOON

Geophysical Fluid Dynamics Laboratory/NOAA, Princeton University, Princeton, NJ 08540

(Manuscript received 5 January 1982, in final form 28 April 1982)

ABSTRACT

The adjustment of the eastern coastal zone of an inviscid ocean with vertical walls to a change in wind conditions occurs in two stages. After the propagation of a Kelvin wave across the forced region in a time T_K which is of the order of a day or two, the coastal upwelling zone is temporarily in equilibrium with the wind. Further adjustment occurs after a time T_R, which is of the order of a few months, when westward Rossby dispersion of the coastal jet becomes important. These time scales define three frequency ranges that characterize the response to fluctuating winds with period P. 1) At high frequencies ($P \leqslant T_K$) short Kelvin waves can destroy coherence between the forcing and response, alongshore coherence of oceanic variables is small, and the spectrum of the response is red even if that of the forcing is white. The offshore scale of the response is the radius of deformation. Poleward phase propagation at Kelvin wave speed c in unforced regions and at speed $2c$ in the forced region is prominent in this frequency range and at all lower frequencies. 2) At intermediate frequencies ($T_K \ll P < T_R$) long Kelvin waves from the boundary of the forced region establish an equilibrium response so that the ocean and atmosphere are practically in phase, but Kelvin waves excited by remote winds could destroy this coherence. Alongshore correlations are high and the spectrum of the response is much less red than at higher frequencies. The offshore scale exceeds the radius of deformation and increases with decreasing frequency. 3) At low frequencies ($P \geqslant T_R$) the offshore scale is the distance Rossby waves travel in time P. A complex system of northward and southward currents appears near the eastern boundary of the basin. It is proposed that the California Current system is generated in this manner.

1. Introduction

Eastern boundary currents such as the California, Canary, Peruvian and Benguela Currents advect cold, high-latitude water equatorward. This, however, does not explain the low sea surface temperatures associated with these currents because the temperatures do not decrease monotonically with increasing latitude. In the southeastern Pacific Ocean, for example, temperatures are at a minimum off the coast of Peru. Coastal upwelling must be invoked to explain the observed sea surface temperature variations (Wooster, 1970). But what is the relation between eastern boundary currents which have an offshore scale of hundreds of kilometers, and coastal phenomena which have an offshore scale of tens of kilometers?

Winds parallel to a coast drive a jet and cause intense coastal upwelling within a radius of deformation of the coast (Charney, 1955; Yoshida, 1955). These features persist as long as the latitudinal gradient of the Coriolis parameter—the β effect—is negligible. Once the vorticity imbalance associated with the advection of fluid particles from high to low latitudes becomes important, then the coastal jet disperses into Rossby waves (Anderson and Gill, 1975; McCreary 1977, 1981). (Physically this is analogous to the dispersion of a vortex such as a Gulf Stream Ring, into Rossby waves.) In the wake of the Rossby dispersion there is steady Sverdrup flow (with no distinctive features near the coast) provided the winds remain steady after their sudden onset. Fluctuating winds, on the other hand, induce a distinctive coastal response. The offshore scale of this coastal region depends on the time scale of the winds. It is the purpose of this paper to determine how the coastal response, and in particular its offshore scale, depends on the period of the forcing.

One of our principal results is that time-dependent winds parallel to a coast, even if their curl is zero, create a source of vorticity in the surface layers of the ocean near the coast. The Rossby waves excited in this manner give rise to a complex system of equatorward and poleward flowing currents near the coast. We propose this as an explanation for the highly variable California Current System which can have three southward flowing tongues separated by northward flow (Hickey, 1979). Mean flow, driven by the curl of the wind stress, is presumably superimposed on these variable currents. In the case of the very wide, slow Peruvian Current the mean flow is more prominent but it is still subject to large perturbations. These perturbations, which Wooster (1970) describes as a complex system of currents, undercurrents and countercurrents, could be Rossby

0022-3670/82/080862-18$08.50

waves excited indirectly by the wind parallel to the coast.

This paper describes the response of an ocean basin that extends from the equator to 30°N. The meridional winds that force motion are spatially uniform between 10 and 20°N and are zero elsewhere. The distance of the forced region from the equator is far greater than the equatorial radius of deformation (which is ~300 km) so that equatorial effects are unimportant in the upwelling region. At the same time the forced region is in sufficiently low latitudes for Rossby waves to be important on relatively short time scales. The unforced region poleward of 20°N permits a study of the effects of nonlocally generated Kelvin waves. A numerical shallow water model of an ocean with vertical walls and a flat bottom (Appendix A) is used for a detailed study (Section 3) of how the oceanic response changes when the period of the sinusoidally varying winds change. A multilevel numerical model (Appendix B) is used to determine the oceanic response to the sudden onset of steady, uniform winds (Section 2), and the response to forcing at periods of 20–200 days (Section 4). The results are discussed and summarized in Section 5.

2. Response to the sudden onset of winds

Before discussing the response to fluctuating winds, it is necessary to determine the characteristic time scales of the oceanic adjustment after the sudden onset of steady winds. There are three distinct phases in the evolution of equilibrium conditions. During the first two stages, discussed in Sections 2a and 2b, the latitudinal variation of the Coriolis parameter is negligible. During the third and final stage (Section 2c), the β-effect is important. Some of the results described here have been derived previously by Charney (1955), Yoshida (1955) and Allen (1976) for a one-level model, Crepon and Richez (1982) for a two-level ocean, and McCreary (1981) and Yoon and Philander (1982) for a stratified ocean.

a. Phase I

Immediately after the onset of the winds alongshore variations are negligible and the wind stress τ^y (which acts in a surface layer of depth H) drives an accelerating coastal jet, i.e.,

$$v_t = \tau^y/H. \tag{1}$$

This is the meridional momentum equation at the coast ($x = 0$) if diffusive effects are negligible. (The coordinates t, x, y and z measure time, and distance eastward, northward and upward, respectively; u, v and w are the corresponding velocity components.) Since the flow is two-dimensional, offshore Ekman drift is balanced by coastal upwelling:

$$u_x + w_z = 0. \tag{2}$$

The associated slope of the isotherms near the coast is in geostrophic balance with the meridional jet. The width of the surface jet is the radius of deformation

$$\lambda = N_0 H/f,$$

where N_0 is a typical value for the Brunt-Väisälä frequency. The structure of the jet is independent of the structure of vertical baroclinic modes and is unchanged should the ocean be infinitely deep.

b. Phase II

Poleward propagating Kelvin wave fronts excited initially at the southern extreme of the forced region establish alongshore variations and change the flow completely. For example, the acceleration of the jet stops because an alongshore pressure gradient P_y balances the wind stress. At the coast ($x = 0$) where $u = 0$ the meridional momentum equation is simply

$$P_y/\rho_0 = \tau^y/H. \tag{3}$$

Compare this equation with (1). The Kelvin waves also introduce an undercurrent, in a direction opposite to that of the surface jet because, in a stratified fluid, the Kelvin waves extend to depths greater than that of the surface jet of depth H.

A further effect of Kelvin waves is to reduce the intensity of the coastal upwelling. This happens because divergence of the coastal jet compensates for the offshore Ekman drift. In a one-level model upwelling ceases completely, and the continuity equation changes from (2) to

$$u_x + v_y = 0. \tag{4}$$

In an N-layer inviscid model in which f is constant, each of the N baroclinic Kelvin waves reduces the upwelling until there is none after the passage of the Nth mode. In a continuously stratified fluid friction must be invoked to cope with the very high order modes so that some upwelling persists (Yoon and Philander, 1982; McCreary, 1981).

Kelvin waves do not modify the u velocity component perpendicular to the coast. This means that the onshore flow at depth, which maintains the upwelling and offshore surface flow during phase I, supplies the coastal undercurrent after the passage of the Kelvin waves.

c. Phase III

The final phase in the establishment of equilibrium conditions is associated with the dispersion of the coastal jet into Rossby waves (Anderson and Gill, 1975; McCreary, 1977). The dispersion is effective after a time $O(T_R)$ where

$$T_R = 4\pi f/\beta c. \tag{5}$$

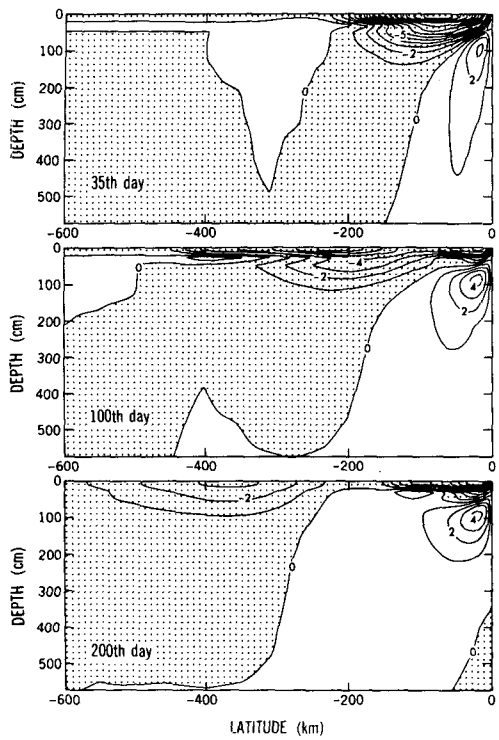

FIG. 1. Zonal section of meridional currents across 15°N in response to steady southward winds of intensity 1.0 dyn cm^{-2}, that suddenly start to blow at day zero. The flow (cm s^{-1}) is southward in shaded areas.

Here c ($=\sqrt{gh}$) is the gravity wave speed in shallow water of depth h, f the local value of the Coriolis parameter and β its latitudinal derivative. (T_R is the maximum period at which Rossby waves are possible in the shallow water model and corresponds to the frequency at which the zonal group velocity is zero.) T_R depends on $\tan\theta$ (where θ is latitude) so that it increases almost linearly with latitude in the tropics. Its value at 45°N is ~100 days if we assign c the value 2 m s^{-1}.

Equilibrium conditions occur in the wake of the westward travelling Rossby waves. In an inviscid shallow water model forced by uniform winds τ^y there is ultimately no motion at all because a pressure force P_y exactly balances τ^y. [The balance in Eq. (3) now obtains everywhere, not only at the coast.] If the winds vary spatially so that curl τ is non-zero then the equilibrium state in the wake of the Rossby waves corresponds to a Sverdrup balance (Lighthill, 1969).

Shallow-water models do not give information about changes in the vertical structure of the flow. We therefore used the multi-level numerical model described in Appendix B to study the evolution of the flow in a stratified fluid after the sudden onset of southward, steady winds of intensity 1.0 dyn cm^{-2}. A surface coastal current and undercurrent evolve during the first few weeks as described above. Subsequently (see Fig. 1) there is westward dispersion, and two southward flowing tongues form in the surface layers. The time-longitude plots along 15°N at 10 m and 70 m (Fig. 2) show this clearly. It is evident from Fig. 1 that the vertical scale, especially that of the coastal undercurrent, decreases with time. To understand why this happens, consider a description of the coastal current and undercurrent that exist during the early stages, in terms of a sum of vertical baroclinic modes. The gravest modes, such as the first and second baroclinic modes, are associated with large vertical scales and high westward group velocities. These modes propagate away from the coast first. After their departure the vertical scale of the coastal current and undercurrent has decreased, and continues to do so as more modes propagate away.

Since Rossby waves propagate more rapidly in low than high latitudes the westward dispersion of the coastal jet should be more advanced in low than high latitudes. Fig. 3a shows that this is indeed the case.

In an inviscid model the equilibrium state in the wake of the westward Rossby dispersion is a state of no motion with a meridional pressure force that

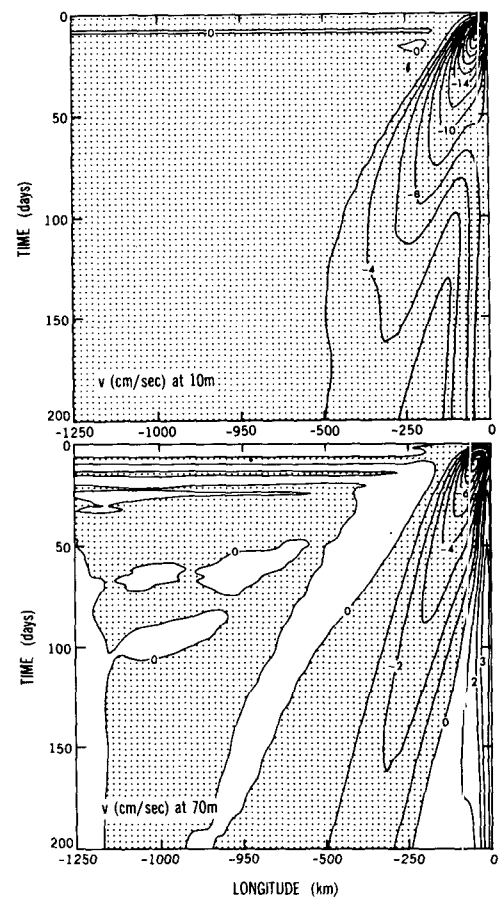

FIG. 2. The evolution of the flow in Fig. 1 at two depths along 15°N.

exactly balances the wind stress (which is a body force). In the presence of dissipation there are steady currents in the final equilibrium state. Fig. 3 shows how these currents can change when the parameterizations of the mixing processes changes. In Fig. 3a the eddy viscosity is Richardson-number-dependent as described in Appendix B. In Fig. 3b the eddy viscosity has a constant value of 10 $cm^2\ s^{-1}$.

3. The response of a shallow-water model to periodic forcing

Two time scales, T_K and T_R, are important in the response of the ocean to the sudden onset of winds parallel to a meridional coast. T_K is the time it takes a Kelvin wave to propagate to the region of interest from the southern edge of the forced region, i.e., $T_K = L/C \approx 2$ days, where L is the distance the Kelvin wave travels—we take this to be 500 km—and c is the gravity wave speed. (In reality L probably depends on the coherence scale of the wind, or it could be the distance from a cape that excites Kelvin waves.) T_R, defined in Eq. (5), is the time for Rossby dispersion to be important. Its latitudinal dependence suggests that a comparison of the variability of eastern boundary currents off the coasts of Oregon and Peru, for example, should be valuable.

The oceanic response to sinusoidally varying winds, $\tau^y \sin(2\pi t/P)$, depends on the magnitude of the period P relative to T_K and T_R. Let us first consider high frequencies.

a. $P \ll T_R$

At these high frequencies Rossby dispersion is unimportant and the β-effect can be disregarded. For these periods the offshore scale of the coastal phenomena is the radius of deformation $\lambda = c/f$. We assume that f is constant and that the meridional velocity component has the form

$$v = c^{-1}\xi(y, t)e^{fx/c}. \tag{6}$$

Then the function ξ can be shown to satisfy the following equation provided diffusive effects are neglected (Gill and Clark, 1974):

$$\xi_t + c\xi_y = \frac{c\tau^y}{H}\sin\left(\frac{2\pi}{P}t\right). \tag{7}$$

The solution to this equation is composed of two parts: a propagating Kelvin wave and a directly wind-driven jet, i.e.,

$$\xi(y, t) = F(y - ct) + \frac{Pc\tau^y}{2\pi h}\cos\left(\frac{2\pi}{P}t\right). \tag{8}$$

The arbitrary function F is the Kelvin wave and can be determined from the boundary condition at the southern extreme of the forced region. For the sake of simplicity we assume that a wall exists there, at

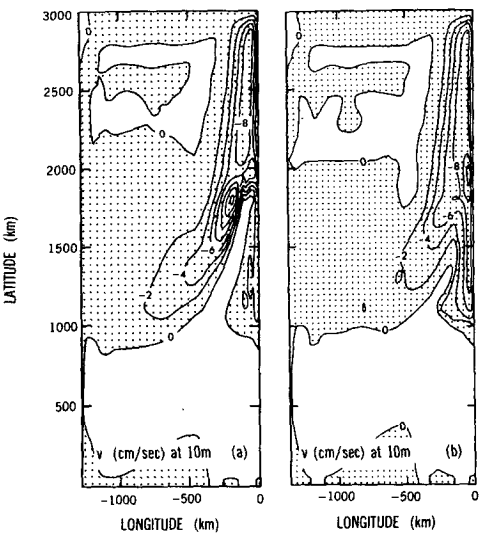

FIG. 3. The meridional velocity component at a depth of 10 m, 150 days after the sudden onset of steady winds in a model in which (a) vertical mixing is Richardson Number dependent as described in Appendix B, and (b) vertical eddy viscosity has the constant value of 10 cm^2/s^{-1}.

$y = 0$:

$$\xi = 0 \quad \text{at} \quad y = 0$$

$$F(-ct) = -\frac{Pc\tau^y}{2\pi h}\cos\left(\frac{2\pi}{P}t\right), \tag{9}$$

$$\xi = \frac{Pc\tau^y}{\pi H}\sin\left(\frac{\pi}{Pc}y\right)\sin\left[\frac{\pi}{Pc}(y - 2ct)\right], \tag{10}$$

$$\rightarrow \frac{y\tau^y}{H}\sin\left[\frac{\pi}{Pc}(y - 2ct)\right] \text{ when } P \gg T_K = \frac{2y}{c}. \tag{11}$$

The unforced region to the north is affected by Kelvin waves from both extremes of the forced region of width l. In this unforced region

$$\xi = \frac{Pc\tau^y}{\pi H}\sin\left(\frac{\pi l}{Pc}\right)\sin\left[\frac{2\pi}{Pc}\left(y - ct - \frac{l}{2}\right)\right].$$

These solutions have several intriguing features.

(i) The amplitude of the response depends on the period of the forcing. At high frequencies the amplitude is linearly proportional to P but for large values of P the factor $\sin(\pi y/Pc)$ comes into play and the amplitude becomes independent of P. This means that if the wind has a white spectrum—if the different Fourier components of the fluctuating wind have the same amplitude—then the response of the ocean is red at high frequencies but is white at low frequencies. The transition occurs in the neighborhood of the time scale T_K defined above. This is a result for the forced and unforced region.

(ii) The meridional velocity component vanishes at nodal points $y = nPc$ where n is an integer. The

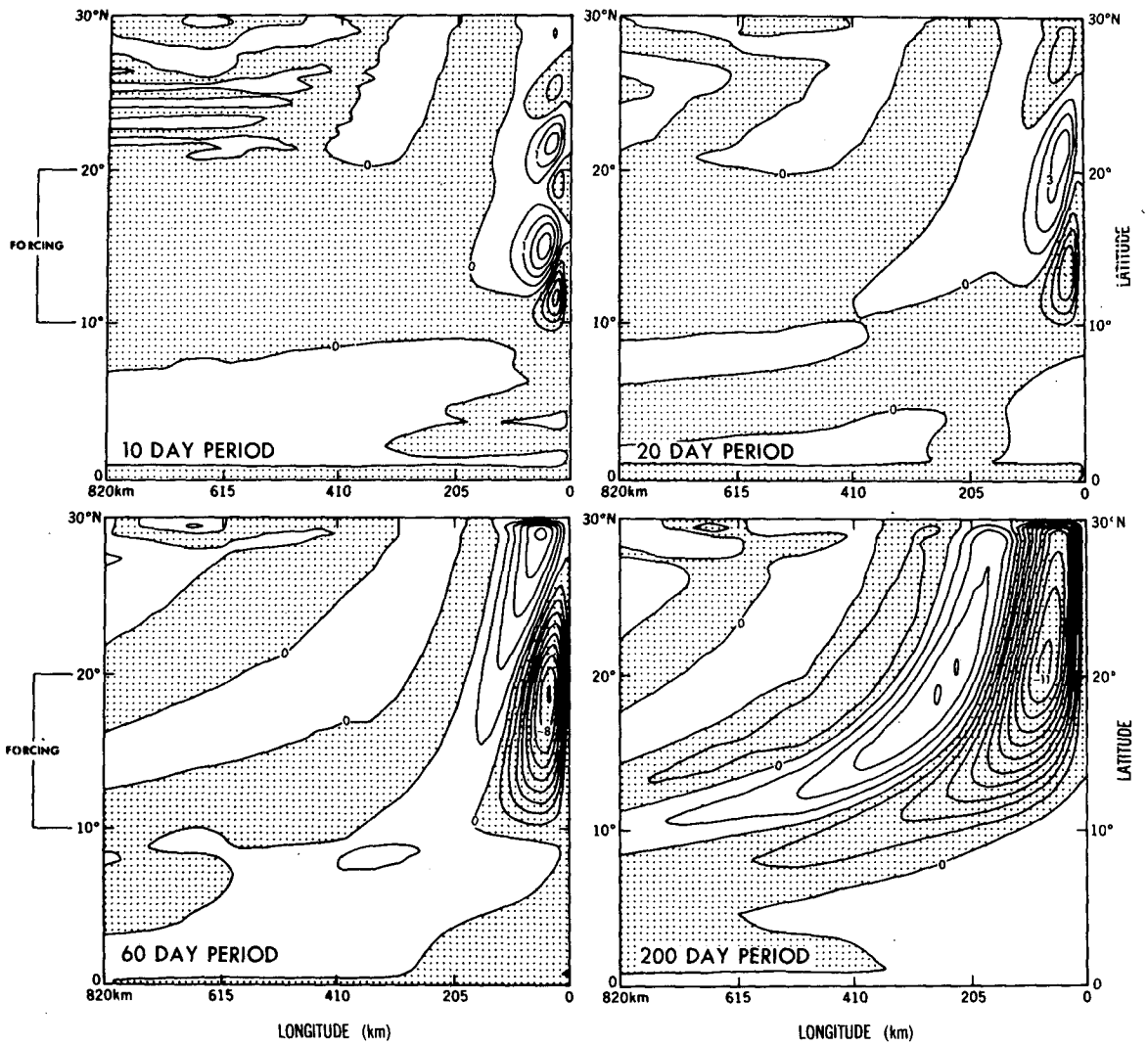

FIG. 4. The meridional velocity component in a shallow water model forced with periodic winds, at the time when the winds are southward and are at a maximum. (This happens after one-quarter cycle.) Flow is southward in the shaded area.

distance between nodal points increases as the period increases. This happens because the wavelength of the Kelvin waves increases as the period increases. The implication is that measurements at points along the coast will be increasingly coherent as the period increases.

(iii) Phase propagation along the coast is at *twice* the Kelvin wave speed c in the forced region but at speed c in the unforced region. The phase speed is $2c$ when the free wave, which travels with speed c, is superimposed on the forced, oscillatory coastal jet.

Fig. 4 shows the meridional velocity component, after ¼ cycle, in a shallow water model (see Appendix A) forced with periodic winds. The winds are southward during the first ½ cycle. Even though friction is important in the model, and even though f varies, the various features just pointed out are clearly evident. Note the increase in both amplitude and in alongshore scale, as the period increases. At a period of 60 days, and especially 200 days, the offshore scale exceeds the radius of deformation. This is attributable to the non-zero value of β [which, in Eq. (8), is assumed to be zero]. The β-effect permits Rossby waves with frequency σ and zonal wavenumber k. For small meridional wavenumbers the dispersion relation is

$$k = \frac{1}{2}\left[-\frac{\beta}{\sigma} \pm \left(\frac{\beta^2}{\sigma^2} - \frac{4}{\lambda^2}\right)^{1/2}\right].$$

The imaginary part of k is k_i where

$$k_i^2 = \frac{1}{\lambda^2}\left(1 - \frac{\beta^2\lambda^2}{4\sigma^2}\right).$$

At high frequencies $k_i \sim \lambda^{-1}$ so that the offshore scale is the radius of deformation. As the frequency

decreases, the e-folding distance increases until it is infinite when Rossby waves become possible at frequency $\sigma = \beta\lambda/2$. This low-frequency range will be discussed later. The main point here is that the offshore scale exceeds the radius of deformation even at frequencies too high for Rossby waves to be possible.

The time-latitude plots along a meridian 40 km from the eastern coast (Fig. 5) clearly show the different northward phase speeds, $2c$ in the forced region (1100 km $< y <$ 2200 km) and c north of the forced region ($y >$ 2200 km). Note that alongshore gradients are small for an observer moving with speed c in the unforced region, but are large in the forced region irrespective of the frame of reference. This result can be inferred from (11). At low frequencies the amplitude of ξ varies linearly with latitude y in the forced region but in the unforced region the amplitude depends only on the width l of the forced region.

According to (10) the meridional velocity component is in phase with the wind and lags by an amount $y/2c$ in the forced region. (The same is true of the pressure and offshore velocity component.) At a fixed latitude y this lag, measured in dimensional time units, is independent of period. If the lag is expressed in radians (as a fraction of the forcing period) then the lag decreases as the period increases. The scale for the ordinates in Fig. 5 has been chosen to illustrate this. (Once Rossby dispersion becomes important the phase relations between the forcing and response change, as we shall shortly show. The response at a period of 200 days is affected by this.)

Eq. (10) implies coherence between the forcing and response at all frequencies but this should not be expected in reality. Our model has an unrealistic nodal point at the southern extreme ($y = 0$) of the idealized forcing region. The absence of such a point in reality—atmospheric storms move—means that Kelvin waves will be excited almost everywhere so that any region is subject to both local *and* remote forcing.

The term "local forcing" does not imply coherence between the local response and the local wind. Suppose that there is forcing only in a certain region, and that the southern boundary of this forced region moves randomly with time. Under such conditions the response in the forced region may not be coherent with local forcing. At high frequencies short Kelvin waves generated at the southern boundary will destroy coherence. If the spatial scale of wind fluctuations were too large to excite short waves then capes and bays along the coast could excite these waves. At low frequencies the long Kelvin waves that are excited have a different effect. Recall that in the initial value problem (Section 2) Kelvin waves introduce equilibrium conditions. If the winds are periodic then at long periods P the Kelvin waves cross

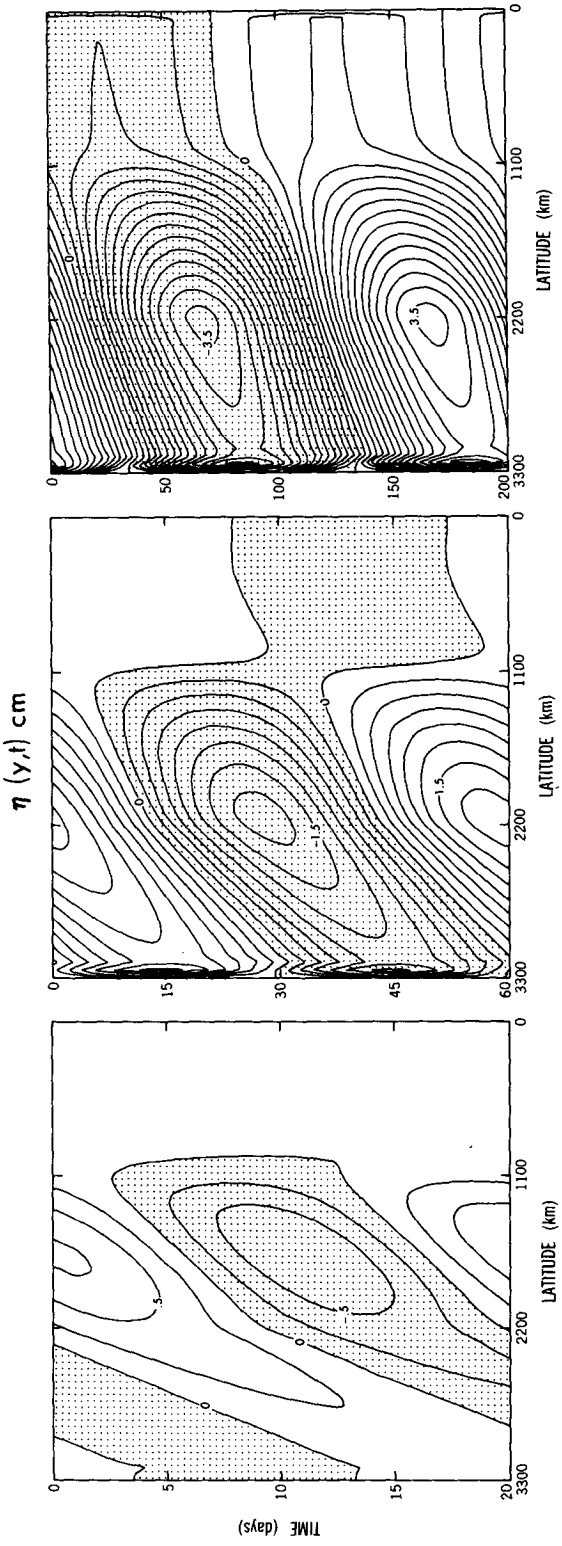

FIG. 5. Thermocline displacements along a meridian 40 km from the eastern coast when the winds over the shallow water model have periods of 20, 60 and 200 days.

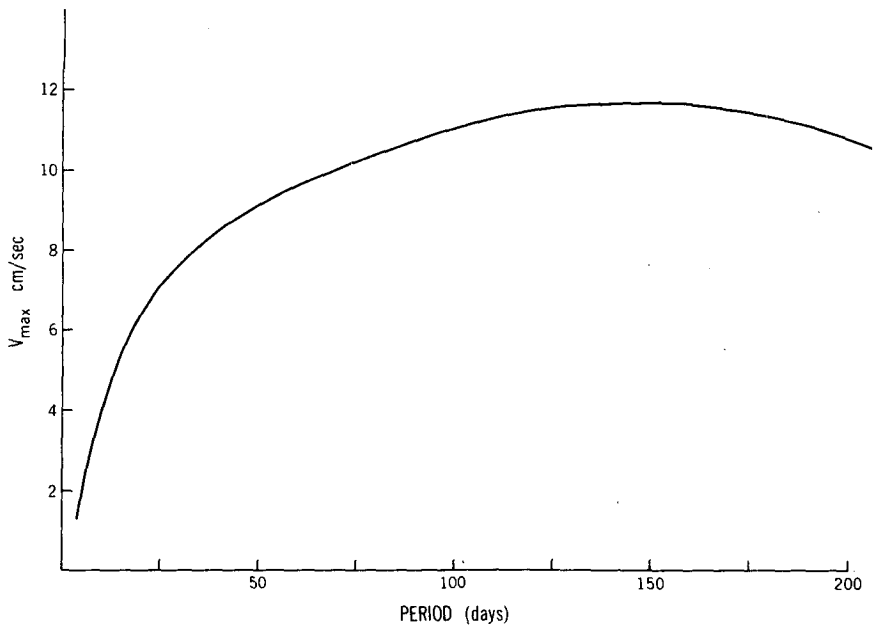

FIG. 6. The maximum amplitude of the meridional velocity component as a function of the period of the wind in the shallow water model.

the forced region in a time short compared to P so that the forced region is at all times in an adjusted state and hence is in equilibrium with the winds. Eq. (11) describes this equilibrium response which lags behind the wind by an amount $Y/2c$.

Although coherence between the forcing and response is possible at low frequencies, nonlocal forcing can still be important. Hence a time-series can have events almost in phase with the local winds and, in addition, events not correlated with the local winds. Since the absence of coherence between forcing and response does not necessarily mean that the forcing is remote, additional tests are necessary to distinguish between the two types of response. Different alongshore phase speeds and different alongshore gradients are two such tests.

After the sudden onset of winds, there is a time ($<T_K$) when the motion is two-dimensional, and offshore Ekman drift is sustained by coastal upwelling. It does not follow that periodic winds with a short period ($P < T_K$) will force two-dimensional motion. Kelvin waves, which introduce longshore variations, are possible at *all* frequencies. Hence coastal upwelling induced by fluctuating winds need not be two-dimensional at any frequency. For example, upwelling *and* divergence of the coastal jet compensates for offshore Ekman drift at all frequencies.

b. $P > T_R$

At low frequencies ($P \gtrsim T_R$) Rossby dispersion must be taken into account. It is now convenient to deal with a vorticity equation. If we assume that f and β are both constants, then (Anderson and Gill, 1975)

$$U_{xxt} + \beta U_x - \left(l^2 + \frac{1}{\lambda^2}\right)U_t = \frac{1}{fH\lambda^2}\frac{\partial}{\partial t}(\tau^y). \quad (12)$$

Here meridional variations are assumed to be sinusoidal with wavenumber l, and λ is the radius of deformation. If the β-effect is negligible then solutions decay exponentially with increasing distance from the coast and we regain the coastally trapped solutions described above. Once the β-effect is important, oscillating solutions in x, associated with Rossby waves, are possible. We write the solution as

$$u = \bar{u}\sin\left(\frac{2\pi}{P}t\right) - \bar{u}\sin\left(kx - \frac{2\pi}{P}t\right), \quad (13)$$

where the first term corresponds to the x-independent wind-driven currents in the absence of any coasts, and the second term corresponds to free Rossby waves which are invoked to satisfy the boundary condition $u = 0$ at $x = 0$. The wavelength $2\pi/k$ is determined by the dispersion relation. If the waves are long and nondispersive then

$$u = +\frac{2\tau^y}{fH}\sin\left(\frac{\pi x}{sP}\right)\sin\left[\frac{\pi}{sP}(x + 2st)\right], \quad (14)$$

where the speed of nondispersive Rossby waves is

$$s = \beta/(l^2 + 1/\lambda^2).$$

This expression is not unlike Eq. (10) except that (10) describes variations along the coast whereas

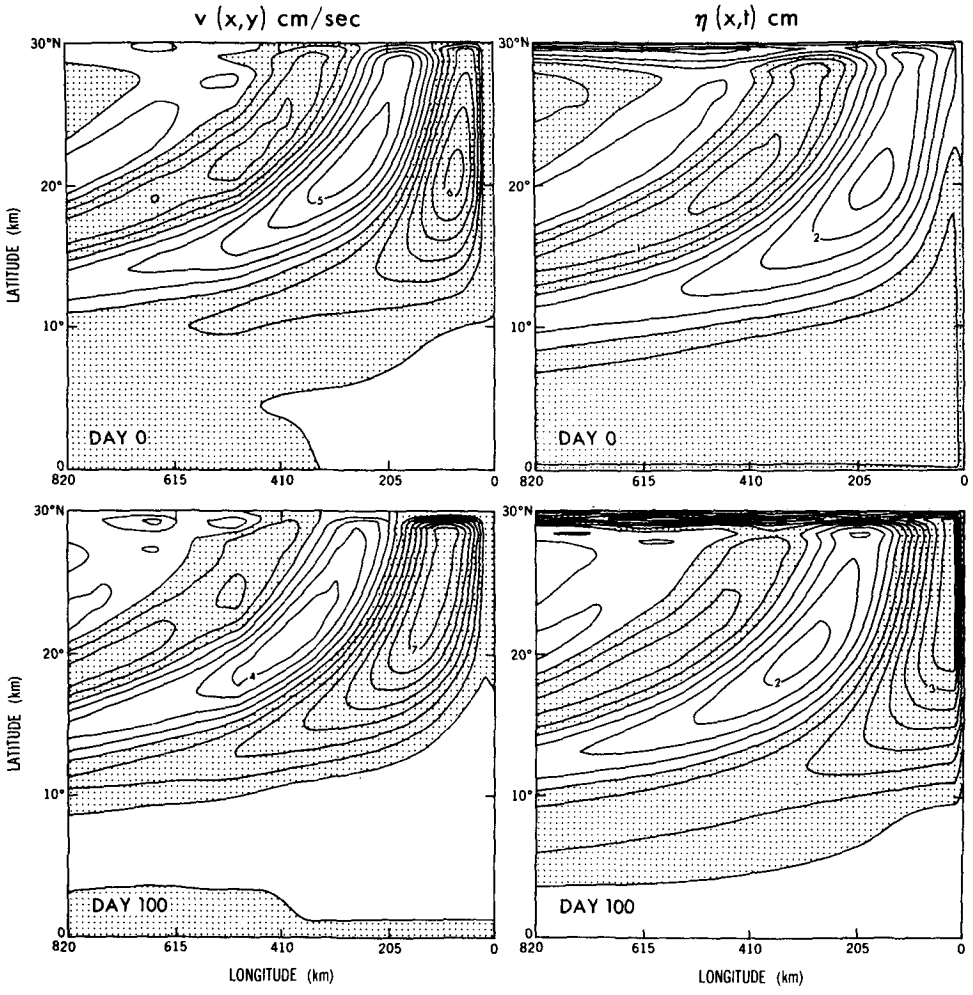

FIG. 7. The alongshore flow and thermocline displacements at days 0 and 100 in a shallow water model forced at a period of 400 days. The winds are southward during the first half-cycle. Flow is southward in the shaded region.

(14) describes variations perpendicular to the coast. A number of interesting results follow from (14):

(i) Westward phase propagation is at the Rossby speed s only in the unforced region. In the forced region phase propagation is at a speed $2s$. (The alongshore velocity component and pressure are not affected in this manner.)

(ii) The amplitude of the response at a fixed distance $\bar{x}$ from the coast is independent of the period at relatively high frequencies ($T_R < P < 2\bar{x}/s$) but at low frequencies ($P \gg w\bar{x}/s$) the amplitude is proportional to $1/P$ as the period P increases. Earlier (Section 3a) we showed that at high frequencies the amplitude increases as P increases and then becomes independent of P. Fig. 6 shows the maximum amplitude of the meridional flow as a function of period P, near 20°N in the shallow-water model described in Appendix A. Note that the amplitude is never completely independent of P. The decrease in amplitude starts at a period of ~150 days. This period will of course vary with latitude. [Keep in mind that results from the model are affected by diffusion whereas Eq. (14) neglects friction.]

(iii) The motion has a spatial (longitudinal) modulation with a scale

$$L = sP. \tag{15}$$

This is the distance a Rossby wave travels in time P. At 15°N L is ~400 km if P = 200 days. (The latitudinal dependence of L is $\cos\theta/\sin^2\theta$.) This is essentially the width of the alternating currents caused by the Rossby dispersion. See the response at a period of 200 days in Fig. 4. At low frequencies this length scale L replaces the Rossby radius of deformation as the appropriate offshore scale.

As the period P becomes very large, we expect an equilibrium response in which motion is vanishingly small because a meridional pressure gradient η_y exactly balances the wind stress (see Section 2c). From

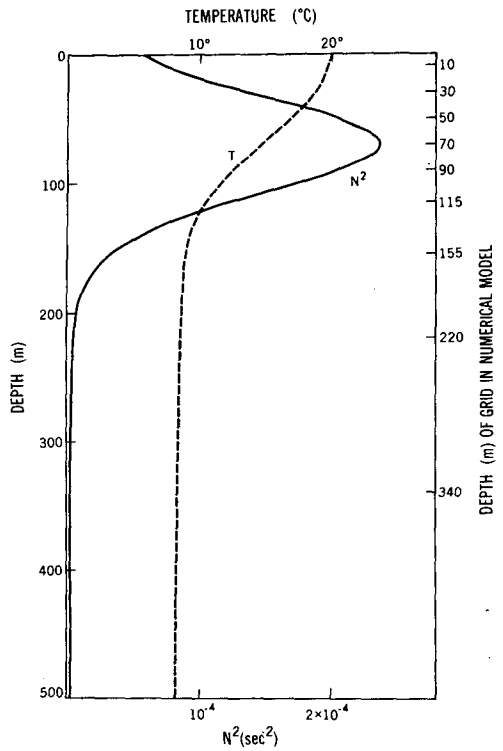

FIG. 8. The initial temperature and Brunt-Väisälä frequency in the multi-level model.

(14) it is evident that these conditions will first be attained close to the coast ($x = 0$). Fig. 5 shows that at a period of 200 days there is still a substantial lag between η_y and the wind. At a period of 400 days (Fig. 7) the lag and the magnitude of the alongshore flow are reduced. This meridional flow is in geostrophic balance, i.e.,

$$fv = g\eta_x .$$

Since x variations are sinusoidal, v is 90° out of phase with the thermocline depth η, and hence with the wind τ^y. This is why, in Fig. 7, the meridional flow leads the wind whereas η_y lags. [McCreary (1977) first discussed these phase relations.]

4. Response of a stratified ocean to periodic forcing

Shallow-water models give no information about the vertical structure of motion and, although they simulate thermocline displacement, they give little information about sea surface temperature variations. We have therefore used a multi-level nonlinear numerical model (see Appendix B) to study the oceanic response to periodic winds. Because such models demand enormous computer resources, our study is confined to forcing at two different periods, 20 days and 200 days. The ocean is initially at rest and is stratified as shown in Fig. 8. (Below 500 m the temperature decreases linearly to zero.) In the absence of any forcing diffusion will cause the temperature profile to change. This happens on a time scale long compared to the time scales of interest here but should nonetheless be kept in mind when inspecting figures that show the evolution of the temperature field. For the chosen initial stratification, the oceanic adjustment is accomplished primarily by the second baroclinic mode, for the reasons given by Philander and Pacanowski (1981). At a depth that corresponds to a node, this mode, of course, is unimportant. In the case where the winds have a period of 20 days, calculations continue for five cycles and results are shown for the fifth cycle. For the case where the winds have a period of 200 days calculations continue for three cycles and results are shown for the third cycle. (Differences between the last two cycles are negligible compared to variations within a cycle.) The winds are southward—favorable for upwelling—during the first half-cycle. Their amplitude is 1.0 dyn cm^{-2}.

a. 20-day period

According to the results in Section 3, Rossby dispersion is unimportant at this period which is almost long enough for the response to correspond to the f-plane equilibrium state of Eq. (11) where the ocean is almost in phase with the wind. Fig. 9 shows that the lag between the wind and the alongshore surface flow is small. The alongshore pressure gradient, however, lags by one-quarter period and is a maximum not when the wind is maximum but at the conclusion of a spell of wind in one direction. As in the shallow-water case poleward phase propagation is greater in the forced region than in the unforced region. This Kelvin wave propagation is evident in all the fields except the near surface temperatures. The reason for this is the dominant effect of Ekman drift on surface temperatures. Note that the lowest temperatures occur at the *end* of the spell of southward winds (day 10). At the end of the spell of northward winds (days 0 and 20) the onshore Ekman drift of warm water has suppressed all sea surface temperature gradients.

Sea surface temperatures hardly vary in the unforced northern region ($y > 2000$ km). The Kelvin waves, however, do affect the subsurface temperatures, and give rise to substantial currents in the unforced region (see Fig. 10). This figure also shows that nonlinear effects are important (otherwise the velocity fields on days 10 and 15 will closely resemble those on days 0 and 5, respectively). At the end of the spell of northward winds (day 0) there exists a strong poleward surface current and a modest equatorward undercurrent in the southern part of the forced region. (The undercurrent is generated by a

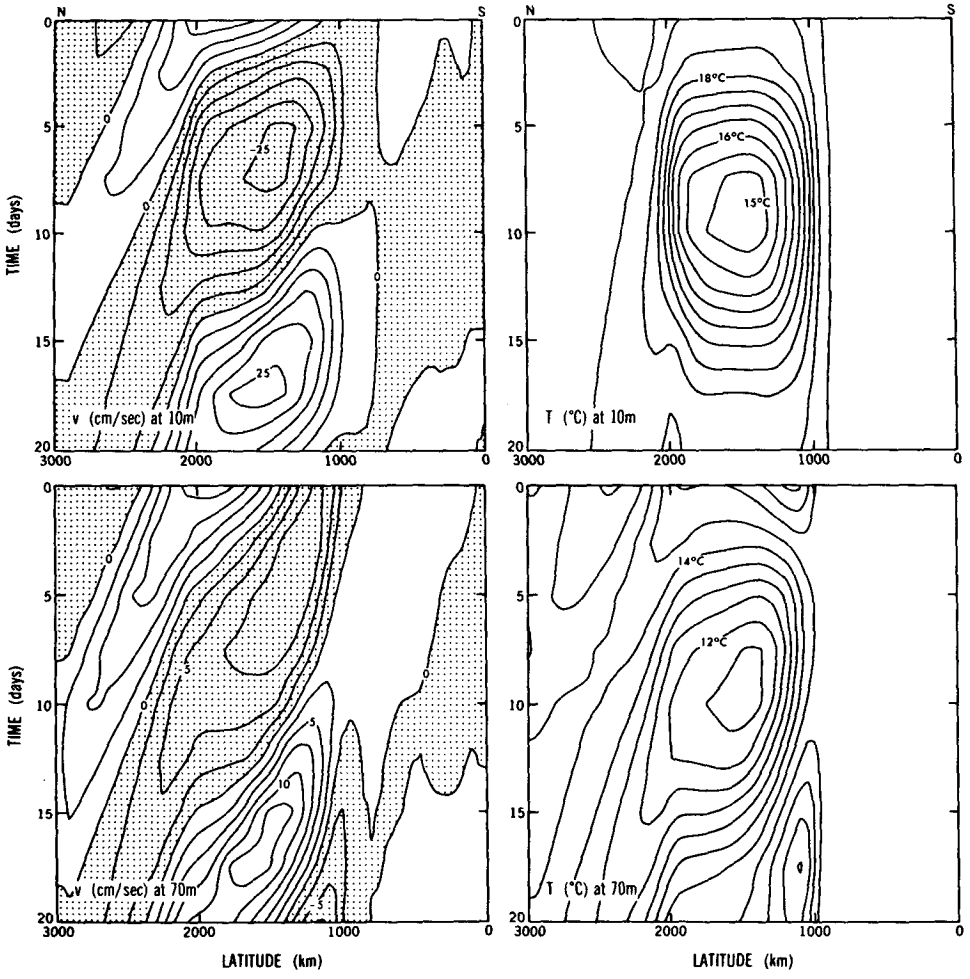

FIG. 9. Meridional velocity and temperature variations at two depths along a meridional 18 km from the eastern coast in response to winds that have a period of 20 days. Winds are southward during the first 10 days. Motion is southward in the shaded regions.

Kelvin wave excited at the southern extreme of the forced region and hence is most intense in the south.) The poleward undercurrent at the end of the period of southward winds (day 10) is much weaker than the corresponding equatorward undercurrent at day 0. The (nonlinear) reason for this is coastal upwelling which advects the poleward momentum of the undercurrent into the surface layers. In Section 3a we argued that in a shallow-water model, at low frequencies ($P > T_K$), divergence of the coastal jet and not upwelling sustains the offshore Ekman drift. In a stratified ocean this result is modified. Consider the response to the sudden onset of steady winds. In a shallow-water model there is precisely one Kelvin wave that suppresses upwelling and establishes equilibrium conditions. In a stratified fluid a large number of vertical baroclinic Kelvin modes each contributes to the establishment of equilibrium conditions. The first few do their share rapidly but the high-order modes travel slowly and have small vertical and offshore scales. Friction dissipates these modes so that the upwelling they should have suppressed, persists. See Yoon and Philander (1982) for a detailed discussion.

Fig. 11 shows the offshore structure of the fields in the center of the forced region at 15°N (a latitude which is poleward of the core of the undercurrent). Note that, at a period of 20 days, the offshore scale is essentially the radius of deformation (30 km at 15°N). The existence of adjacent meridional currents in opposite directions could have been anticipated from the results in Section 3 (see Fig. 4). When the wind starts to blow northward (say) on day 10 there already exists a southward current. The wind-driven northward flow is most intense near the coast so that a northward current appears there while the

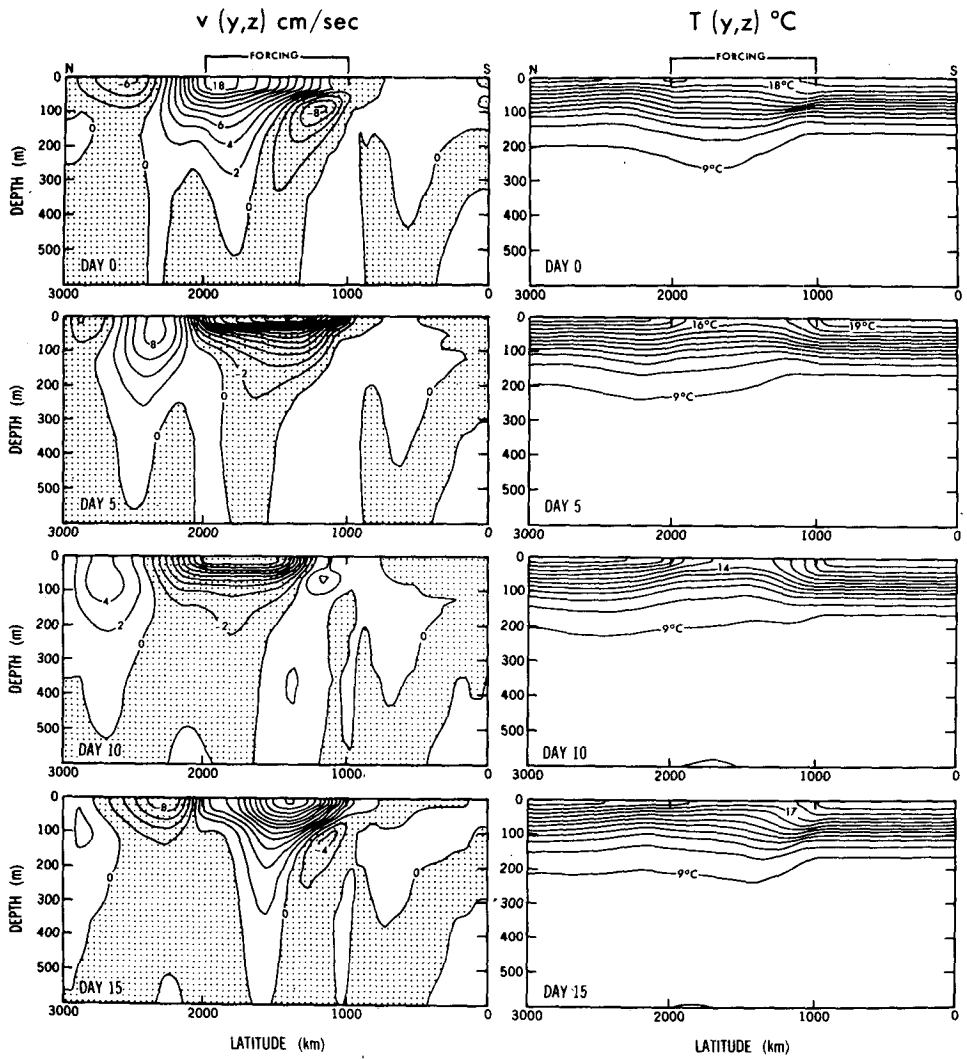

FIG. 10. Meridional sections of the flow in Fig. 9.

flow offshore is still southward (day 15). Because of nonlinear effects this sequence is not merely reversed when the wind blows equatorward. Momentum from the equatorward current close to the coast is advected offshore in the surface (Ekman) layers so that the surface flow is equatorward everywhere on day 5 (which would have resembled day 15 if the motion were linear).

b. 200 days

At a period of 200 days $P > T_R \gg T_K$ so that Rossby dispersion is important. A comparison of Figs. 12 and 11 clearly shows the enormous increase in offshore scale when the period increases from 20 to 200 days. At 20 days the appropriate scale is the radius of deformation, at 200 days it is the distance a Rossby wave propagates in that time. It is evident that nonlinear effects are important, otherwise the velocities at days 0 and 50 would closely resemble those at days 100 and 150, respectively. As in the case of 20-day forcing, the equatorward undercurrent is more prominent than the poleward undercurrent. The reasons are the same as before.

The Rossby dispersion results in the complex system of northward and southward flowing currents shown in Fig. 13. This pattern propagates westward as depicted in Fig. 14 but note that Ekman drift, not Rossby dispersion, determines the sea surface temperature pattern. When the winds are northward and warm surface waters flow toward the coast, there are no sea surface temperature gradients at all. In response to forcing at one period, there is westward phase propagation all along a fixed latitude circle only if f and β are assigned constant values. If f is permitted to vary with latitude then the Rossby

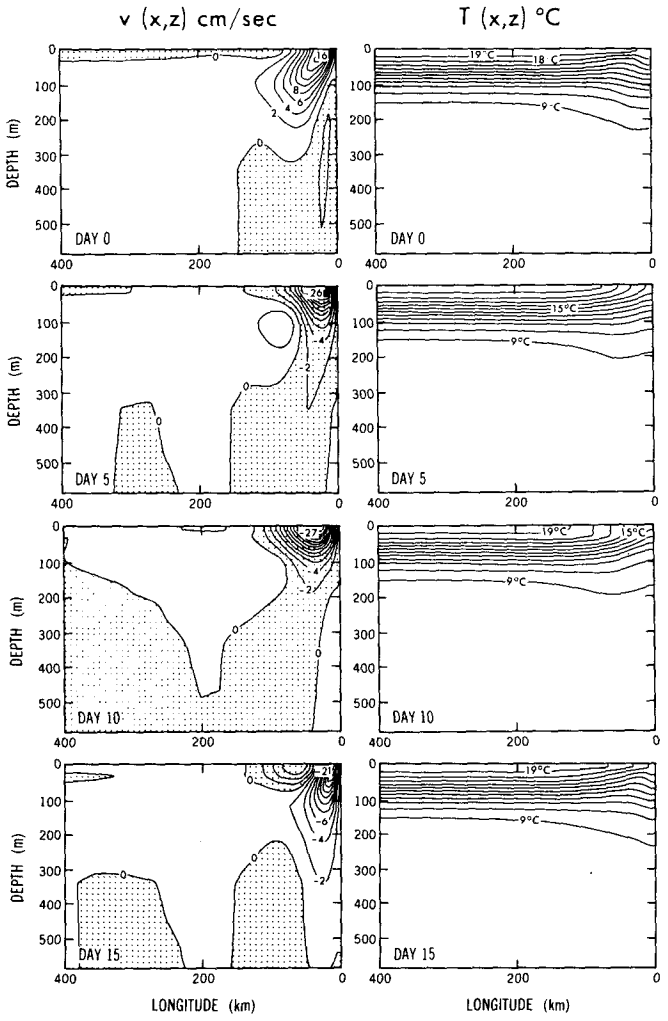

FIG. 11. Zonal sections along 15°N of the flow in Fig. 9.

waves are refracted so that measurements sufficiently far from the coast may not show westward phase propagation. For a detailed discussion of this effect, which is included in our numerical model, the reader is referred to Schopf *et al.* (1981).

A comparison of Figs. 15 and 10 reveals that alongshore pressure gradients are far more important at a period of 200 days than at a period of 20 days. Because of this there are large currents at much greater depths. (At a period of 20 days currents are driven primarily by the winds, not the pressure gradients, and hence are shallower.)

The phase relations between the forcing and the response changes considerably when the period changes from 20 to 200 days. At a period of 20 days all the fields lagged behind the wind, but at 200 days the alongshore velocity component near the coast leads the wind as shown in Fig. 16. (In Section 3b we showed that in the asymptotic state $P \rightarrow \infty$ the currents lead by $\pi/2$ and the alongshore pressure gradients are in phase with the wind.) At the end of a spell of winds in one direction the currents near the coast are in the opposite direction. In Fig. 13 there are southward coastal currents at day 0 after the winds had been northward for 100 days. The southward flow is "downhill" because there is a southward pressure force at day 0. This pressure force is created by the northward wind and can be viewed as the driving force for the coastal undercurrent. At day 50, for example, the northward pressure force is associated with geostrophic motion toward the coast. At the coast the flow turns poleward, in the direction of the pressure force, while the wind drives the surface layers southward. The Equatorial Undercurrent is similarly caused by the eastward pressure force maintained by the westward winds but it is an order of magnitude more intense than the coastal undercurrent. One of the reasons for this is

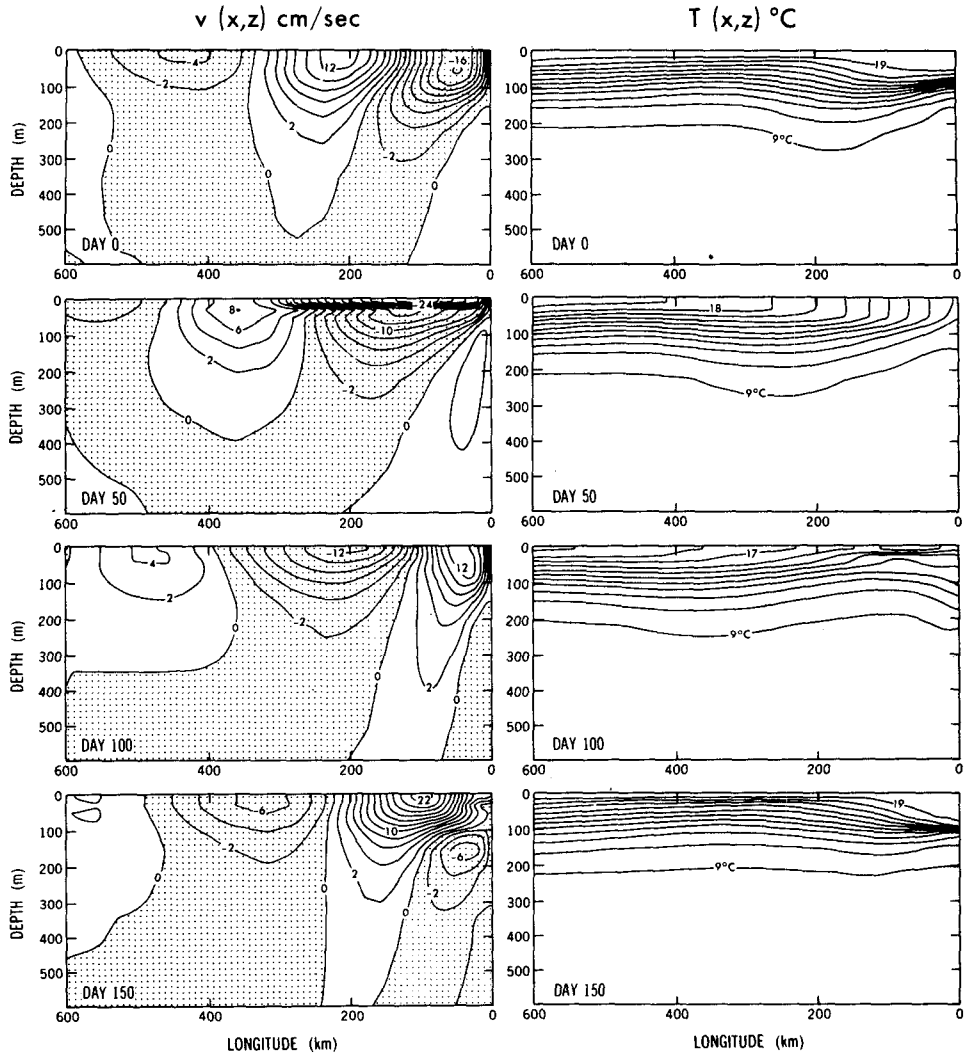

FIG. 12. As in Fig. 11 but the period of the wind is 200 days and winds are southward during the first 100 days.

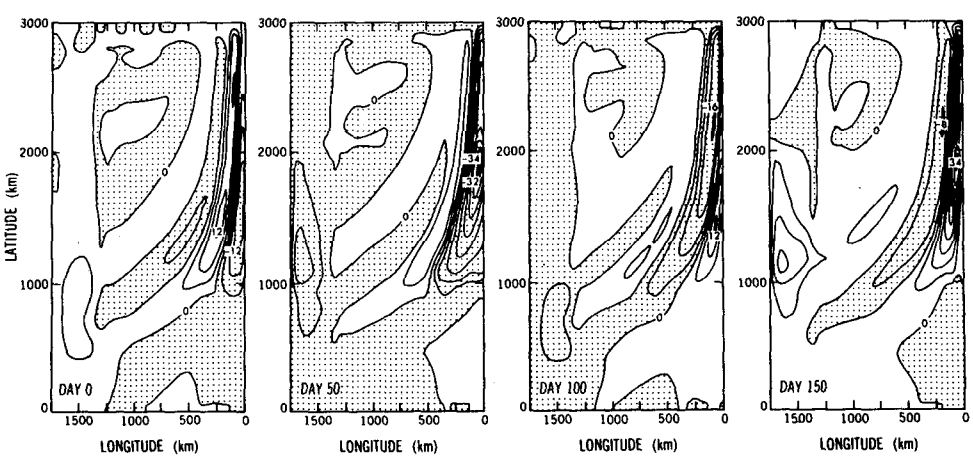

FIG. 13. The meridional velocity component (cm s^{-1})—southward flow in shaded areas—during four stages of the 200-day cycle.

the following. The planetary vorticity of equatorward-moving particles changes rapidly. To conserve their total vorticity the particles accelerate eastward (Fofonoff and Montgomery, 1955). The planetary vorticity of particles that move toward a meridional coast does not change so that there is no intensification of the coastal undercurrent.

5. Summary and discussion

The eastern coastal zone of an inviscid ocean with vertical walls responds to the sudden onset of steady winds as follows. At first alongshore variations are negligible, the wind drives an accelerating coastal jet, and offshore Ekman drift is maintained by coastal upwelling. A Kelvin wave excited at the southern extreme of the forced region changes the flow completely when it arrives after a time T_K: the acceleration of the surface jet stops because alongshore pressure gradients balance the wind, a coastal undercurrent with a direction opposite to that of the wind appears, and upwelling decreases because divergence of the coastal currents helps maintain offshore Ekman drift. In a shallow-water model these changes occur abruptly when a Kelvin wave passes. In a stratified ocean several vertical Kelvin modes could be involved so that the transition is more gradual. The final phase of the oceanic adjustment starts after a time T_R which is of the order of a few months, when Rossby dispersion results in a complex system of southward and northward flowing currents off the eastern coast. The offshore scale which had been the radius of deformation is now the distance Rossby waves travel in a given time.

The case just discussed, where steady winds suddenly start to blow, is highly idealized. In a more realistic situation the winds are fluctuating. Instead of Kelvin wavefronts excited at one instant there are now continuous wavetrains excited all the time. The local oceanic response consists of two parts: directly wind-driven flow plus waves excited at the boundaries of the forced region. The wind-driven part is two-dimensional (independent of the alongshore coordinate) if the winds are uniform, but the Kelvin waves introduce alongshore variations. These waves are possible at all frequencies so that the motion is three-dimensional at *all* frequencies. It has been argued [see Allen (1980) for a review] that inclusion of a constant alongshore pressure gradient permits certain three-dimensional problems to be solved with two-dimensional models. The results presented here suggest that this cannot be done when the winds fluctuate over a spectrum of frequencies. It is noteworthy that several authors, Huyer (1976) and Smith (1978) for example, have emphasized that the observed mass balance near coasts is three-dimensional.

The purpose of the Kelvin waves is to establish

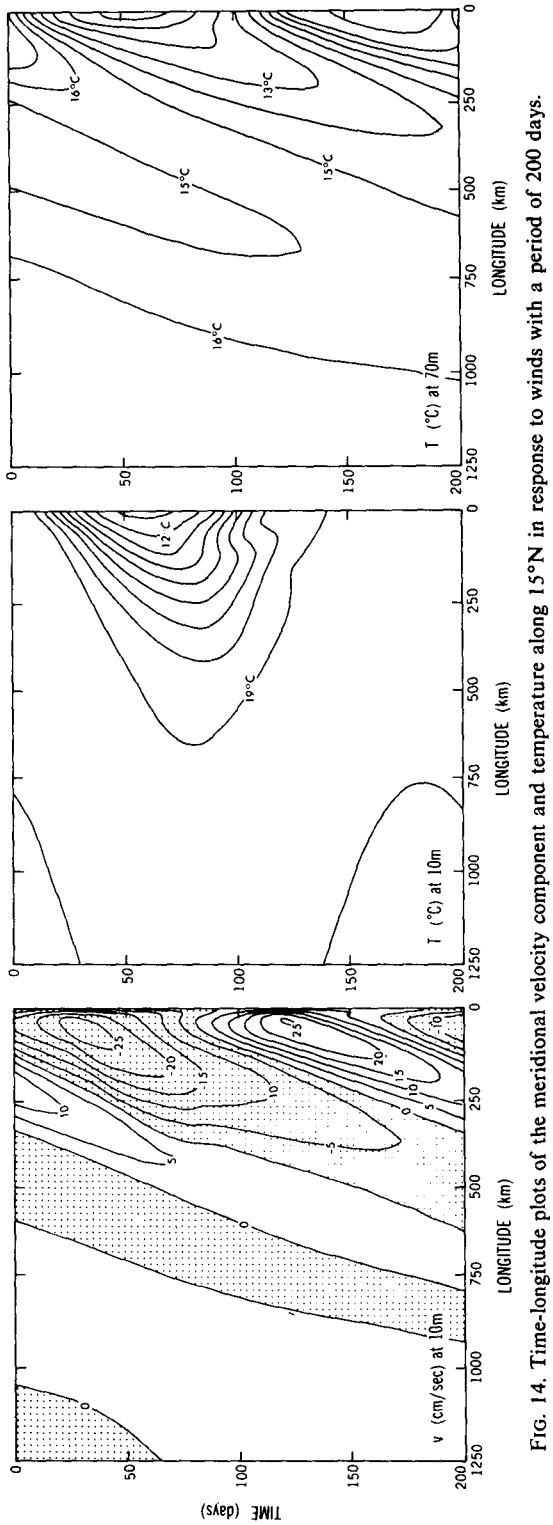

FIG. 14. Time-longitude plots of the meridional velocity component and temperature along 15°N in response to winds with a period of 200 days.

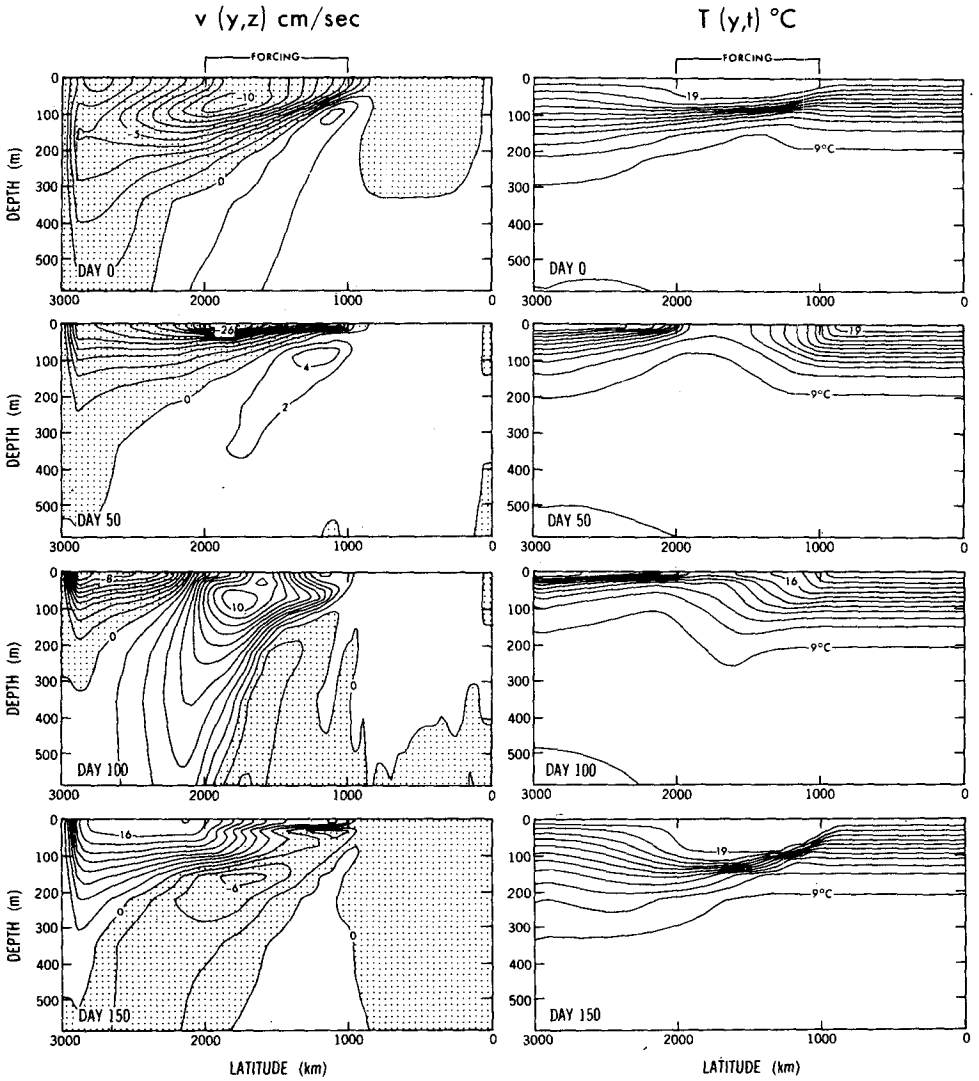

FIG. 15. Meridional sections of the flow at a distance of 18 km from the eastern coast when the winds have a period of 200 days.

alongshore pressure gradients and thus to bring the ocean into equilibrium with the winds. This is clearly evident in the case where steady winds start to blow suddenly. When the fluctuating winds have a long period P which greatly exceeds the time T_K it takes Kelvin waves to propagate across the forced region, then the ocean is practically in equilibrium with the wind and the forcing and response are almost in phase. When the period P is too short for this to happen then the short Kelvin waves that are excited destroy coherence between the forcing and response. Hence, at high frequencies correlations between the wind and oceanic motion is unlikely. If the spatial scale of wind fluctuations is too large to excite short Kelvin waves then capes and bays along the coast could excite short waves. [Portolano (private communication, 1981) finds that in the upwelling zone just north of Dakar, where the African coast has a prominent cape, high-frequency oceanic variability is uncorrelated with the local winds.] At low frequencies $T_R > P \gg T_K$ correlations are possible but could be destroyed by Kelvin waves excited in distant regions. In general, lack of coherence between the forcing and response does not imply that the motion is forced by remote winds.

Measurements along a coast should be increasingly coherent as the period increases because the wavelengths of the Kelvin waves increase. The measurements should also show poleward phase propagation, at the long gravity wave speed c if the disturbances are forced by remote winds, but at speed $2c$ if the disturbances are locally forced. Given the considerable spatial and temporal variability of the density near a coast, it is difficult to determine from

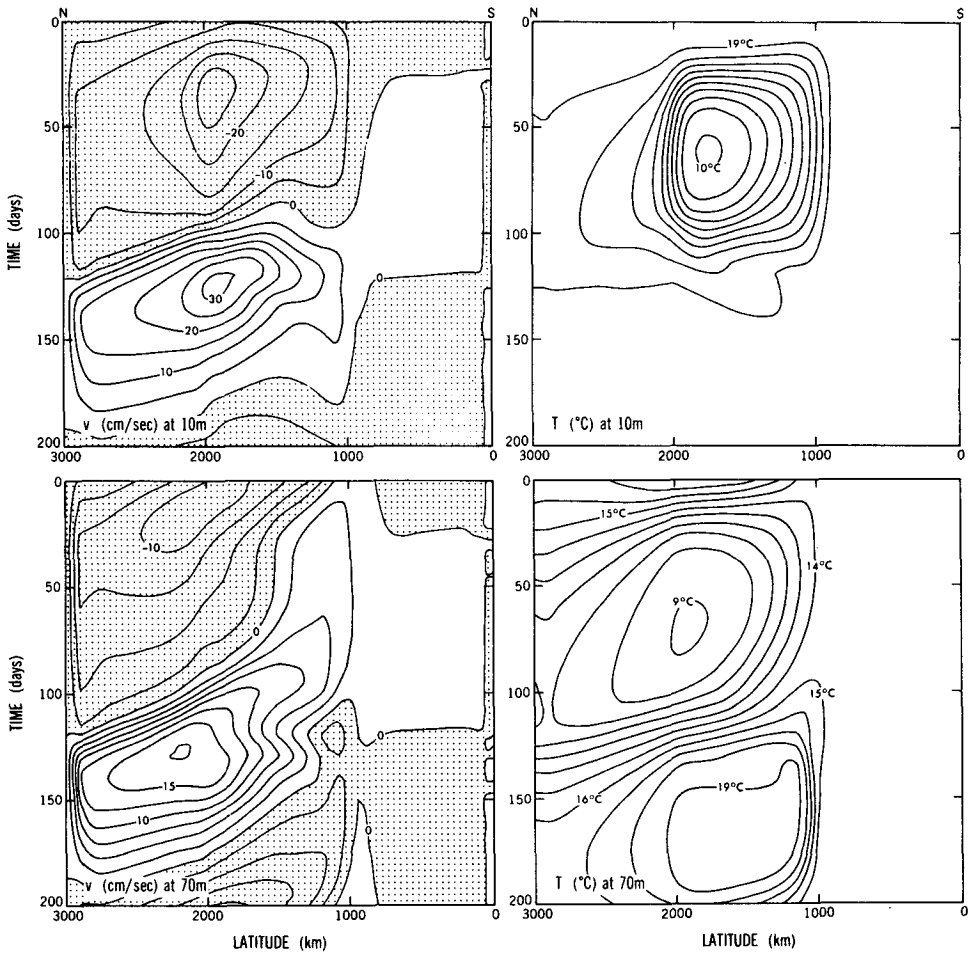

FIG. 16. Meridional velocity and temperature variations at two depths along a meridian 18 km from the eastern coast.

measurements what the appropriate value for c is. Hence measurements that show phase propagation at a speed that is reasonable for Kelvin waves are probably indicative of a superposition of waves and local wind-driven currents.

At long periods $P > T_R$ the offshore scale is no longer the radius of deformation but is the distance Rossby waves propagate in the time P. A complex system of westward propagating, northward and southward flowing currents appear off the eastern boundary of the ocean basin. The wind, even though its curl is zero, in effect provides a source of vorticity in the surface layers of the ocean near the coast. The curl of the wind happens to have a large value just off the western coast of North America (White and Saur, 1981). Calculations with realistic winds are necessary to determine the relative importance of the curl of the wind, and the component of the wind parallel to the coast in generating eastern boundary currents and Rossby waves.

This discussion has emphasized the importance of two inviscid time scales (T_K and T_R). The numerical models that have been used include diffusive processes which affect the structure of the currents significantly. However, the characteristic time scales of the model response are not affected by diffusion. If dissipation in the model had been much larger so that frictional time scales are comparable to T_K then the oceanic response would be different. Allen (1980) discusses this response when dissipation is dominant. Certain parts of the ocean, especially very shallow shelf regions, are very turbulent but further offshore the flow is essentially inviscid (Brink *et al.*, 1978). The extent to which the dissipative shelf region will affect the inviscid adjustment described here needs to be studied by including topographic effects into a stratified model.

This paper has described the oceanic response to very idealized wind-stress patterns. In reality the wind has a complex spatial and temporal structure.

Irregular coasts which have capes and bays introduce even more complexity. This suggests that coastal upwelling should be studied not only as a sequence of events, but also as a stochastic phenomenon. To do this it will be necessary to obtain long time-series of oceanic variables as measured at points along the coast and at points along a line perpendicular to the coast.

Acknowledgments. We thank Ms. Seigel for considerable assistance with the computations, Ms. Williams for typing the manuscript, and Mr. Tunison and his staff for drafting the figures. This work was supported by Geophysical Fluid Dynamics Laboratory/NOAA Grant 04-7-022-44017.

APPENDIX A

The Shallow Water Model

The linear shallow-water equations are solved numerically by means of finite differencing methods on a C-grid (Holland and Lin, 1975). Horizontal velocity components vanish at the vertical coasts. The rectangular basin extends from the equator to 30°N and is 1850 km wide. The 57 × 60 grid points are irregularly spaced. Resolution is highest near the eastern coast where the grid spacing is 6.2 km for a distance of 100 km from the coast. The spacing then increases gradually until it reaches a maximum value of 51.7 km. The latitudinal spacing is regular and is 51.7 km. The horizontal diffusion, which has a Laplacian form, is variable. Its value is 10^7 cm^2 s^{-1} within 500 km of the eastern coast, then increases gradually near the western coast where the value is 10^9 cm^2 s. This highly diffusive region near the western boundary prevents disturbances generated there (Kelvin waves, for example) from propagating to the eastern side of the basin.

The (equivalent) depth of the model is 15 cm so that the gravity wave speed is 123 cm s^{-1} and the radius of deformation at 15°N is 35 km.

Initially the ocean is at rest. The periodic winds prevail for 10 cycles. Figs. 4–7 show results for the tenth cycle. The winds are southward—favorable for upwelling—during the first half-cycle.

APPENDIX B

The Multi-Level Model

The rectangular ocean basin is 2000 m deep, 1760 km wide and extends 3000 km northward from the equator. The zonal grid spacing is 6 km for a distance of 90 km from the eastern coast and then increases gradually to a maximum value of 50 km near the western coast. The latitudinal spacing is a uniform 50 km. The irregular vertical spacing in the upper part of the ocean is shown in Fig. 8. The total number of levels in the model is 12.

Vertical mixing is Richardson Number (Ri) dependent, i.e.,

$$\nu = \left[\frac{50}{(1 + 5\ \mathrm{Ri})^2} + 1\right] \mathrm{cm}^2\ \mathrm{s}^{-1},$$

$$\kappa = \left[\frac{\nu}{1 + 5\ \mathrm{Ri}} + 0.1\right] \mathrm{cm}^2\ \mathrm{s}^{-1},$$

where

$$\mathrm{Ri} = \beta g T_z/(U_z^2 + V_z^2),$$

$$\beta = 8.75 \times 10^{-6}(T + 9),$$

and T is the temperature (°C). This choice for vertical mixing is explained in Pacanowski and Philander (1982).

The horizontal mixing is 10^7 cm^2 s^{-1} for momentum, 10^6 cm^2 s^{-1} for heat except near the western coast where these values are increased by a factor of 100 in order to dampen any disturbances generated there.

The ocean floor is stress-free but velocity components vanish at the vertical walls. A meridional wind stress is imposed at the ocean surface in a 1000 km wide zonal band which is 1000 km from the equator. The heat flux is zero at the boundaries except the surface where

$$T_z = \gamma(T^* - T),$$

where γ is 70 ly(°C day)$^{-1}$ and T^* is 19.6°C. The initial stratification is shown in Fig. 8. Below 500 m the temperature decreases linearly to zero at the ocean floor. The equivalent depths for the first two baroclinic modes are 15.2 and 6.5 cm. The associated gravity wave speeds are 122 and 80 cm s^{-1} and the radii of deformation are 18 and 12 km.

REFERENCES

Allen, J. S., 1976: Some aspects of the forced wave response of stratified coastal regions. *J. Phys. Oceanogr.*, **6**, 113–119.

——, 1980: Models of wind-driven currents on the continental shelf. *Annual Review of Fluid Mechanics*, Vol. 12, Annual Reviews, Inc., 389–433.

Anderson, D. L. T., and A. E. Gill, 1975: Spin up of a stratified ocean with applications to upwelling. *Deep-Sea Res.*, **22**, 583–596.

Brink, K. H., J. S. Allen and R. L. Smith, 1978: A study of low frequency fluctuations near the Peru coast. *J. Phys. Oceanogr.*, **8**, 1025–1041.

Charney, J. G., 1955: The generation of oceanic currents by winds. *J. Mar. Res.*, **14**, 477–498.

Crepon, M., and C. Richez, 1982: Transient upwelling generated by two-dimensional atmospheric forcing and variability in the coastline. Submitted to *J. Phys. Oceanogr.*

Fofonoff, N. P., and R. B. Montgomery, 1955: The Equatorial Undercurrent in the light of the vorticity equation. *Tellus*, **7**, 518–521.

Gill, A. E., and A. J. Clark, 1974: Wind-inducted upwelling, coastal currents and sea-level changes. *Deep-Sea Res.*, **21,** 325–345.

Hickey, B. M., 1979: The California Current System: hypotheses and facts. *Prog. Oceanogr.*, **8,** 191–279.

Holland, W. R., and L. B. Lin, 1975: On the generation of mesoscale eddies and their contribution to the oceanic general circulation. *J. Phys. Oceanogr.*, **5,** 642–657.

Huyer, A., 1976: A comparison of upwelling events in two locations: Oregon and Northwest Africa. *J. Mar. Res.*, **34,** 531–546.

Lighthill, M. J., 1969: Dynamic response of the Indian Ocean to the onset of the southwest monsoon. *Phil. Trans. Roy. Soc. London*, **A265,** 45–92.

McCreary, J. P., 1977: Eastern Ocean response to changing wind systems. Ph.D. thesis, University of California, San Diego, 156 pp.

——, 1981: A linear stratified model of the coastal undercurrent. *Phil. Trans. Roy. Soc. London*, **A302,** 385–413.

Pacanowski, R., and S. G. H. Philander, 1982: Parameterization of vertical mixing in numerical models of the tropical oceans. *J. Phys. Oceanogr.*, **11,** 1443–1451.

Philander, S. G. H., and R. C. Pacanowski, 1981: The generation of equatorial currents. *J. Geophys. Res.*, **85,** 1123–1136.

Schopf, P., D. L. T. Anderson and R. Smith, 1981: Beta-dispersion of low frequency Rossby waves. *Dyn. Atmos. Oceans*, **5,** 187–214.

Smith, R. L., 1978: Poleward propagating perturbations in current and sea levels along the Peru coast. *J. Geophys. Res.*, **79,** 435–443.

White, W. B., and J. F. T. Saur, 1981: A source of annual baroclinic waves in the eastern subtropical North Pacific. *J. Phys. Oceanogr.*, **11,** 1452–1462.

Wooster, W. S., 1970: Eastern boundary currents in the South Pacific. *Scientific Exploration of the South Pacific.* W. S. Wooster, Ed., Natl. Acad. Sci., Washington, DC, 60–68.

Yoon, J. H., and S. G. H. Philander, 1982: The generation of coastal undercurrents. *J. Oceanogr. Soc. Japan* (in press).

Yoshida, K., 1955: Coastal upwelling off the California coast. *Rec. Oceanogr. Works, Japan*, **15,** 1–13.